Journal of Electronics and Electrical Engineering
https://ojs.wiserpub.com/index.php/JEEE/

Research Article

Evaluation of a HVDC Interconnection to Improve the Voltage Stability of the Nigerian Transmission Network

Omowumi G. Olasunkanmi[1], Andrew R. Barron[1], Alvin Orbaek White[1,2], Grazia Todeschini[3*]

[1] Energy Safety Research Institute, Swansea University, Bay Campus, Swansea, UK
[2] TrimTabs Ltd, Swansea, UK
[3] Department of Engineering, King's College London, Strand Campus, Strand, UK
[*] Correspondence: grazia.todeschini@kcl.ac.uk

Received: 6 November 2023; **Revised:** 17 December 2023; **Accepted:** 27 December 2023; **Published:** 22 January 2024

Abstract: The Nigerian transmission network is prone to outages and low reliability, and both issues are currently impacting the population's quality of life and hindering economic development; this situation is expected to worsen in the future due to the increase in forecasted demand. This paper assesses the stability of the Nigerian transmission network under existing grid conditions, and determines the impact of High Voltage Direct Current (HVDC) on voltage stability. The PV and QV analysis methods were carried out using the DIgSILENT PowerFactory software package. Two weak buses were identified, and an HVDC model was built and integrated into the existing network at these locations. The results demonstrated that the HVDC interconnector positively impacts system stability by improving the voltage profile and the Reactive Power Margin (RPM).

***Keywords*:** critical demand, reactive power margin (RPM), stability analysis, VSC-HVDC, PV analysis, QV analysis

1. Introduction

The continuous growth of electricity consumption and the introduction of renewable energy sources, combined with the difficulty and cost of building new transmission lines, pose increasing demands on power systems worldwide. As a result, modern power systems have been compelled to operate close to their stability limits, which may result in voltage instability or collapse [1, 2]. The availability of a stable and reliable electricity grid is a crucial driver of economic growth and societal change, particularly in developing economies, such as Nigeria. In this context, power system planning is essential for making informed decisions about energy investment for future grid development [3, 4]. While waiting for such developments, electricity providers in Nigeria must increase the use of existing transmission facilities due to the constantly increasing load demand [5]. The Northern part of the country is particularly affected by poor voltage profile due to insufficient dispatch and control infrastructure, radial and fragile system topology, frequent system collapse, and exceedingly high transmission losses. The country's generation stations are spread out across a large area, and unacceptable voltage drops on the network are observed, due to long-distance electricity transmission. As a result, voltage collapse may result from even minor disruptions [6–8]. Consequently, studying voltage stability is crucial for a safe and dependable power supply.

Copyright ©2024 Omowumi G. Olasunkanmi, et al.
DOI: https://doi.org/10.37256/jeee.3120243799
This is an open-access article distributed under a CC BY license
(Creative Commons Attribution 4.0 International License)
https://creativecommons.org/licenses/by/4.0/

In general terms, power system stability is the ability of an electric power system to regain a state of operating equilibrium after being subjected to a physical disturbance [9, 10]. Stability analysis allows identifying a power system operation that provides energy to consumers at an acceptable voltage and frequency with the lowest possible cost [11, 12].

Within the broad range of stability studies, this paper focuses on static voltage stability analysis to evaluate the voltage stability and loadability margins under the current and future demand levels. Static analysis will offer insightful information to determine the voltage magnitude at different points and the increased load demand on the power system. This information is critical to ensure that the voltage levels remain within acceptable limits and preventing voltage collapse. This research aims to evaluate the system's steady-state voltage stability under various operating situations and to locate the voltage collapse points. Static voltage stability analysis is conducted to identify the weak areas regarding the system's reactive power shortage and ascertain the crucial contingencies of voltage stability margins.

Various approaches are used in static voltage stability analysis, including modal analysis, optimization method, continuation load flow method, Power-Voltage (PV) curves, and Reactive-Voltage curves (QV) method (also known as nose curves). PV and QV curves are among the most popular static voltage stability analysis methods, and they are adopted in this work [1]. A PV curve is a graph that shows the relationship between active power (P) and voltage magnitude (V) at each busbar. In contrast, the QV curve is a graphic representation of the relationship between the reactive power (Q) injected into or consumed by a power system and the corresponding voltage (V) at each busbar [13]. The ability of PV and QV curves to accurately give information such as power limits, critical voltage, and stable and unstable operation areas has made them become effective tools for static voltage stability analysis [1, 13, 14]. More specifically, these curves allow the identification of weak buses, with the tendency to experience voltage instability or a limited ability to maintain a steady voltage level under certain operating conditions. Weak buses are characterized by having low voltage magnitude, often close to the voltage collapse point [15].

Given the continuous growth in demand and the difficulties related to developing new transmission lines, numerous researchers have investigated using power electronic equipment to improve power system stability. Power electronics are growing in popularity due to the improved performance and reduced cost observed in the last decade. Using IEEE benchmark models (14-bus, 30-bus, and 118-bus test systems), a new line voltage stability index (BVSI) was used in [2] to identify weak lines and buses on various loading conditions and network configurations. An analytical approach was applied to determine the optimal location of reactive power compensation placement, which was used to improve system voltage stability with current and increased demand. Other work [16] used a Multi-Criteria Decision Making (MCDM) method on the same test systems to improve the voltage stability by optimizing the location of the facts controller. This increased the loading margin and reduced the active power losses. In another paper [17], DIgSILENT PowerFactory (DSPF) was used to identify the weak bus in the IEEE-14 bus system. PV and QV curves allowed for determining the weak bus for Static Var System (SVS) placement. In this way, demand and load margin were improved [17]. The impact of a Voltage Source Converter High Voltage Direct Current (VSC-HVDC) was studied in [15], and it was concluded that this device stabilizes the system voltage as loads continuously change. As the connected loads are further increased, VSC-HVDC generates reactive power to support the AC system, increase capability and stabilize the AC voltage [15]. Further research on voltage stability improvement was conducted by controlling the active power flow via a VSC-HVDC in [18]. It was concluded that if the VSC-HVDC link is heavily loaded and a power system disturbance occurs, a decrease in DC power allows the VSC-HVDC to keep supporting the AC voltage [18].

In [19], both a VSC-HVDC and a conventional AC transmission line were considered for reinforcement in a transmission system that was significantly loaded. According to [19], the first alternative allowed for more power transfer and enhanced the stability of the power system, while lowering the demand for generators to produce reactive power. With a VSC-HVDC link connected between two weak points, the voltage magnitude increased to 0.93 pu; with the AC transmission line, the voltage magnitude was around 0.85 pu [19].

This work aims to conduct a voltage stability analysis on the Nigerian transmission network by using a detailed computer model and applying PV and QV analysis. Next, the impact of a VSC-HVDC on system stability is assessed. This analysis was carried out using data provided by the Nigeria Electricity System Operator (NESO). DSPF was chosen for this research due to its versatility and capability to carry out numerous types of power system studies [20].

The research presented in this paper is part of a larger project investigating the impact of HVDC interconnectors on the Nigerian Transmission system. Given the forecasted increase in demand, it is expected that the transmission system in Nigeria will need to expand. Given the decreasing costs of HVDC technology, this may be a viable solution to replace transmission lines. The impact of HVDC on voltage profile and reliability indices has been addressed in [7, 21], respectively. To the Authors' knowledge, this is the first work where the impact of HVDC connections on the Nigerian Transmission system is studied in detail.

The motivation for performing a stability study is to develop and propose an effective solution to enhance the stability limits of the Nigerian transmission system. This will increase both the system loading and the reactive power margin (RPM). The security margin estimates how much the demand can increase before the system collapse is reached. Consequently, increasing the security margin will reduce the risk of system collapse and allow for future system expansion.

2. Methodology

2.1 *Stability analysis of two buses*

A simple stability analysis of a power system with two buses is presented here, to review fundamental concepts related to this topic. More detailed background information can be found in [22]. The system under consideration is shown in Figure 1, where a transmission line connects two buses (the sending end and the receiving end). A generator is connected to the sending end, and a load to the receiving end, for illustration purposes only. Under the assumption of a lossless transmission line, the line impedance is expressed as $Z = jX$, where X is the line reactance. Based on [23, 24], the equations below are used to determine the system's maximum power (P_{max}) and the critical voltage (V_{crit}), respectively:

$$P_{\max} = \frac{1}{2}\frac{V_1^2}{X}\left(\frac{1}{\cos\phi_2} - \tan\phi_2\right) \tag{1}$$

$$V_{crit} = \frac{1}{\sqrt{2\,(1+\sin\phi_2)}} \tag{2}$$

where P_{max} (MW) is the maximum power, V_1 (pu) is the sending end voltage at the initial condition, and ϕ_2 (rad) is the angle between voltage and current. V_{crit} (pu) is the critical voltage. Equation (1) is known as the maximum system load or the system loadability limit. The system voltage will decline uncontrollably if the load is increased beyond the loadability limit [10]. Therefore, voltage stability analysis is important to determine the system's critical voltage point and the collapse margin. These parameters may be determined using the PV curves and QV curves as described in the next section.

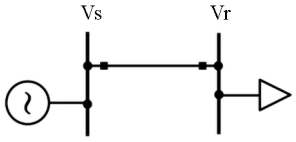


Figure 1. A simple two-bus system

2.2 *PV and QV curves*

After building a computer model of the system under study, the first step to determine PV and QV curves requires a power flow study. This ensures system convergence given the initial generation and load conditions [24, 25]. More details on the load flow analysis carried out for this project can be found in [7].

The PV and QV curves are obtained by increasing the active and reactive power demands. It is noteworthy that active power demands are changed by keeping the reactive power demands fixed when computing the PV curves. Conversely, reactive power values are modified when the active power is kept fixed, when computing the QV curve. For each new demand condition, the load flow analysis is repeated. The corresponding voltage magnitudes and active power values are recorded.

Plotting voltage values against active power levels a graph yields the PV curve, with voltage magnitude on the Y-axis and active power on the X-axis. The resulting curve depicts how the system voltage varies with changes in active power demand. A similar process generates the QV curve, with reactive power values plotted on the X-axis and voltage magnitudes plotted on the Y-axis. This work calculated the PV and QV curves at each busbar, but only the most relevant results will be presented [24].

2.3 *HVDC integration*

At the moment, no HVDC is present on the Nigerian transmission network. Therefore, a separate HVDC model was built and tested separately from the main network. Various control models were considered to determine if they impacted the voltage stability analysis. The details of the HVDC models will be presented in the next section.

The location for the HVDC interconnection was determined based on the PV and QV analysis results. From these results, two cases were studies, where the HVDC was connected between different busbars. Noteworthy, the aim of the analysis was to identify the best HVDC locations that would lead to the most visible improvement in stability analysis, and therefore, only one HVDC was studied at the time.

3. Network model and HVDC model

To carry out the static stability analysis, a model of the Nigerian transmission 330 kV network was built using the electrical and stability data provided by the NESO. The HVDC model was added to the transmission system model at the weak buses identified by the PV and QV studies. In this paper, HVDC technology was studied as a solution to voltage stability concerns, because this work fits within a larger evaluation of HVDC impact on the Nigerian power system. Cheaper and more localized solutions exist for voltage regulation, i.e., FACTs devices such as STATCOMs or VSCs, as highlighted in the literature review [15, 16].

3.1 *Network model*

The power system in Nigeria is divided into four categories: generation, transmission, sub-transmission, and distribution. The network has a total capacity of 14,034 MW, provided by three hydro stations (14.69% of installed generation, 2,062 MW) and seventeen gas stations (85.31% of installed generation, 11,972 MW). The transmission system-rated voltage is 330 kV, while the sub-transmission-rated voltage is 132 kV. The distribution system (demand stage) medium voltage includes 33 kV and 11 kV and the low voltage is 415 V [7].

The network under study consists of 64 transmission lines, including 21 double circuit lines with a total length of 6,575.30 km, 50 bus bars, 20 generators (two of which were out of service based on the data provided), and 22 loads. More details about the Nigerian transmission network can be found in [21], while the transmission network single-line diagram is given in Figure 2.

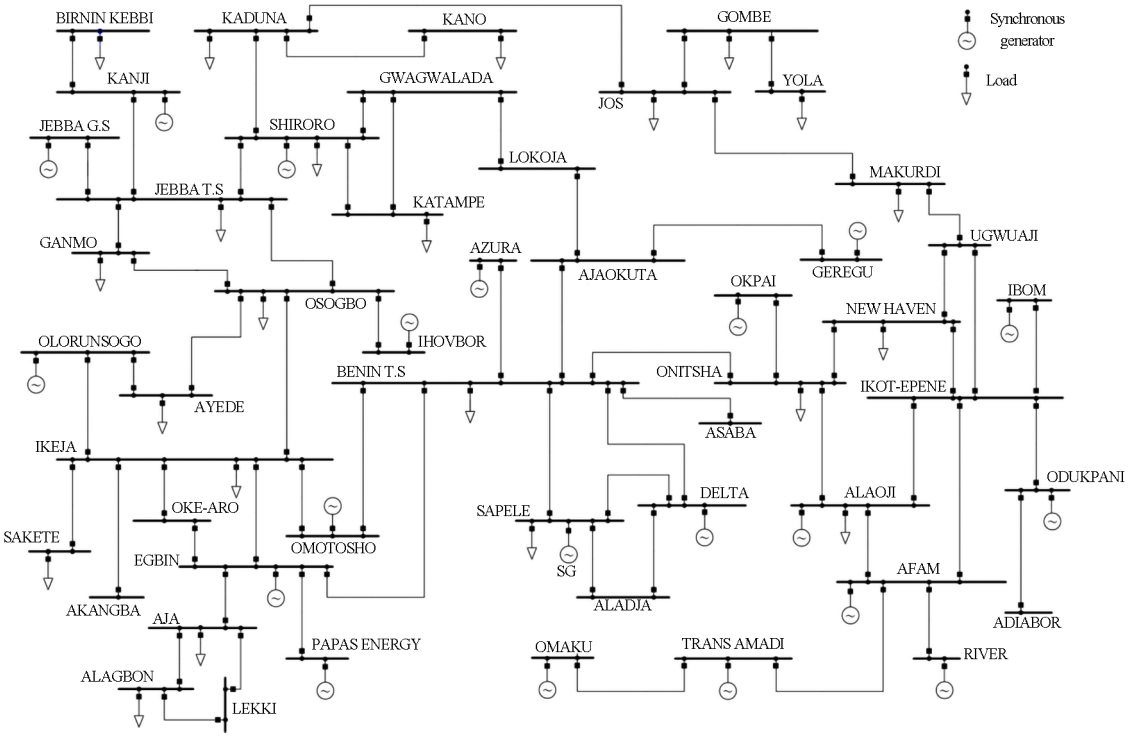


Figure 2. Single line diagram of the nigerian 330 kV transmission network

The Nigeria Energy System Operator (NESO) supplied data for active power demand for each load and generator for both the summer and winter scenarios in 2019. These two cases represent the maximum and the minimum load, respectively [7]. The data provided by the NESO for the stability study includes the active power (P) in MW for each load and for each generator. The load and generator's reactive power was calculated using a power factor between 0.7 and 1. The active and reactive power demand at each load busbar are listed in Appendix Table 11.

3.2 *HVDC model and control*

The model of a VSC-HVDC was built separately to be integrated into the Nigeria transmission system. A VSC-based technology was chosen because it represents the future of HVDC interconnectors. In the rest of the paper, this technology will be called 'HVDC' to simplify the notation. A bipolar topology was considered because it is widely used for long-distance HVDC transmission projects, particularly where high power transfer capacity is required [26]. A rated DC voltage of 500 kV was adopted, based on the distance (approximately 1,000 km for the interconnectors considered in this work) and the rated voltage of the rest of the system (330 kV). A capacitor is used on the DC bus to stabilise the voltage for a balanced actual power exchange between the converter stations, ensuring the proper functioning of the HVDC system. If the active power is not balanced between the two substations, the energy stored in the capacitor decreases or increases.

The converter stations were rated 500 MVA and controlled by pulse-width modulation [27]. PWM control in HVDC systems adjusts pulse width to regulate average voltage or current, enabling efficient long-distance power transmission [25, 28]. The active power was controlled by altering the phase angle of the converter AC voltage with respect to the filter bus voltage, and the magnitude of the fundamental component with respect to the filter bus voltage.

Different HVDC control modes can be deployed to govern and manage the functioning of the sending-end and receiving-end VSCs. These control modes aim to preserve the HVDC system's reliable and effective functioning while achieving different objectives [29]. The control scheme regulates the active power flow from the AC grid to the DC grid and manages the DC voltage to maintain a defined reference level. It also delivers the necessary reactive power to the alternating current mains. This control system comprises two controllers. The first controller regulates the DC voltage,

while the second adjusts the current flow by balancing DC power and AC power [30,31]. The DC voltage control can be explained with the equations below. The reference currents (I_d, I_q) are obtained by the DC voltage controller from the reference real power and reference DC voltage as given below.

$$I_d^* = \frac{P^*}{V_s} + K_v\left(V_{dc}^* - V_{dc}\right) \tag{3}$$

$$I_q^* = 0 \tag{4}$$

where P^* is the reference real power to be transmitted across the HVDC, V_s is the supply voltage, K_v is the proportional gain constant, and $V_{dc}{}^*$ is the reference DC voltage. Reference reactive current (I_q) is taken as zero to maintain a unity power factor.

The reference currents ($I_d{}^*$, $I_q{}^*$) from the DC voltage controller are fed into the AC current controller which provides reference voltages ($V_d{}^*$, $V_q{}^*$) to the PWM block. The operation of the current controller is expressed as follows in the Laplace domain:

$$V_d^* = V_d - \left(R \cdot I_d + sL \cdot I_q\right) - \left(K_p + K_i/s\right)\left(I_d^* - I_d\right) \tag{5}$$

$$V_q^* = V_q - \left(R \cdot I_q + sL \cdot I_q\right) - \left(K_p + K_i/s\right)\left(I_q^* - I_q\right) \tag{6}$$

where K_p is the controller proportional gain, V_d, V_q are the supply voltage dq components and I_d, I_q are the ac current dq components [30]. R and L refer to the output filter parameters.

In this work, the sending end converter was set to control the DC voltage (V_{dc}) and either the reactive power (Q) or the phase angle ($\cos\phi_2$) while the receiving end converter was set to control the active power (P) and either the voltage magnitude (V_{ac}) or the reactive power. As a result, four different combinations can be identified for each converter, leading to the following control modes:

I. V_{dc}–Q/P–V_{ac}: the sending end converter controls V_{dc} and Q; the receiving end converter controls P and V_{ac}.

II. V_{dc}–$\cos\phi_2$/P–V_{ac}: the sending end converter controls V_{dc}, and $\cos\phi_2$ while the receiving end converter controls P and V_{ac}.

III. V_{dc}– $\cos\phi_2$/P–Q: the rectifier controls V_{dc} and $\cos\phi_2$ and the inverter controls P and Q.

IV. V_{dc}–Q/P–Q: the rectifier controls V_{dc}, and Q, while the inverter reference output is P and Q [32]

The adopted model is described more in detail in [21]. Using the control modes described above, the impact of HVDC on system stability was assessed. It is worth noting that the HVDC power flow is unidirectional, as loads are connected to the receiving end in all cases considered.

Results: PV and QV analysis results will be presented in this section, starting with a Base case, where no HVDC is connected to the network. This case allowed the identification of the weakest buses. The impact of HVDC on both PV and QV analysis is then presented for two HVDC interconnectors, identified as Case 1 and Case 2. Results for N-1 contingency are presented at the end of the section.

3.3 *PV analysis-base case results*

The PV analysis was carried out by increasing the real power (MW) transfer from the generators to the loads, as described in Section 2.2. The PV curves obtained for six busbars (Gombe, Jos, Kaduna, Kano, Makurdi, and Yola) are shown in Figure 3. These busbars have been chosen because they are the ones that reach the nose point first. For the

summer scenario, the initial network demand is 4,654 MW. The load flow stops converging when demand reaches the critical value of 5,399 MW: at this condition, all six buses show a voltage magnitude below the acceptable voltage value (0.95 pu). When the network demand is 5,399 MW, Yola (the red line) is identified as the critical bus, having reached the nose curve at a voltage magnitude of 0.66 pu. This result can be explained by observing that Yola lacks voltage regulation equipment and is located at the end of a radial feeder. Gombe (the purple line) too reaches the nose point at 0.69 pu. Additionally, other buses (Jos, Kaduna, Kano, and Makurdi) have voltage drops of 0.81 pu, 0.94 pu, 0.90 pu, and 0.92 pu respectively when the load is increased.

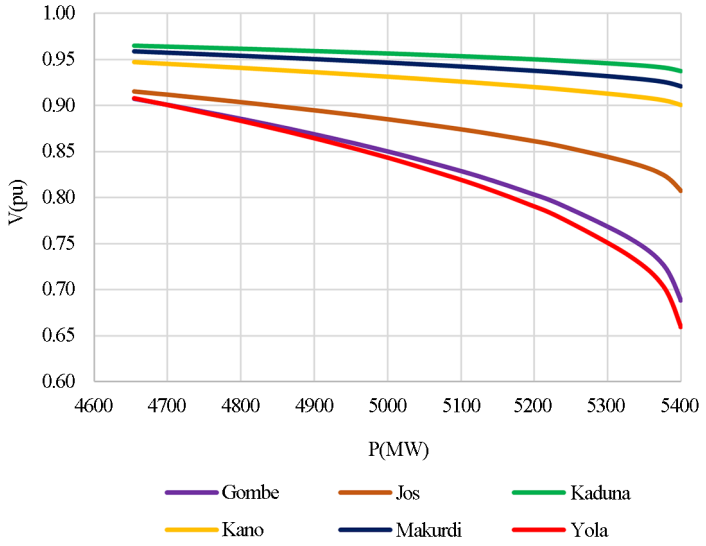


Figure 3. PV curves for the weakest buses for the base case

These values are summarised in Table 1. Kaduna is the bus with the highest critical voltage for both the summer case (0.94 pu) and the winter case (0.97 pu). The lowest critical voltage during both summer and winter are observed at Yola, with values of 0.66 per unit and 0.64 per unit, respectively. Based on the PV analysis, it is concluded that Yola and Gombe are the two weakest busbars as both reach the nose point earlier than Jos, Kaduna, Kano, and Makurdi.

The critical demand during the winter scenario is 5,223 MW, and the Yola and Gombe buses are the weakest, with 0.64 pu and 0.68 pu, respectively. Jos, Kano, and Makurdi buses have voltage drops of 0.86 pu, 0.93 pu, and 0.92 pu, respectively. Table 1 indicates that, generally, the voltage levels are higher in the winter, due to lower load levels compared to the summer. Therefore, for stability analysis, the summer scenario will be considered as the one providing the most conservative results.

Table 1. Voltage magnitude for the weakest buses in the network

	Summer			Winter		
Bus	Load flow voltage (pu)	PV (pu)	QV (pu)	Load flow voltage (pu)	PV (pu)	QV (pu)
Gombe	0.91	0.69	0.5	0.95	0.68	0.46
Jos	0.92	0.81	0.75	0.99	0.86	0.78
Kaduna	0.96	0.94	0.93	1	0.97	0.96
Kano	0.95	0.9	0.91	0.97	0.93	0.93
Makurdi	0.96	0.92	0.92	1.01	0.92	0.89
Yola	0.91	0.66	0.41	0.95	0.64	0.35

3.4 *QV analysis-base case results*

The QV analysis was carried out next to evaluate the impact of reactive power variation on voltage stability.

Figure 4 presents the plot of the critical voltage with the reactive power margin for six buses with a voltage magnitude below 0.95 pu. It is worth noting that these buses are the same as in Figure 3, and therefore PV analysis and QV analysis lead to the identification of the same weak buses. Kaduna and Makurdi show 0.84 pu/−619 Mvar and 0.78 pu/−538 Mvar for critical voltage and reactive power, respectively; while Kano and Jos show 0.55 pu/−204 Mvar and 0.76 pu, / −140 Mvar, respectively. Gombe and Yola show 0.66 pu/−54 Mvar and 0.61 pu/−42.57 Mvar respectively. In this work, positive reactive power means capacitive loads, while negative reactive power refers to inductive loads.

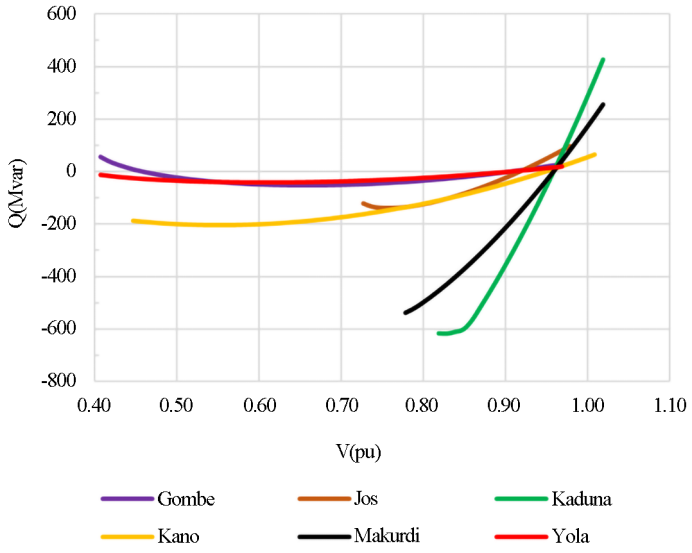


Figure 4. QV curves for the weakest buses for the base case

The bus distance from the generator is important in relation to the capability of the load to absorb reactive power. Kaduna load can absorb high reactive power to maintain the system stability since it is close to the Shiroro generator. Nevertheless, its voltage magnitude is 0.93 pu (Table 1), which is still below the permissible limit of 0.95 pu. Makurdi bus shows a similar pattern. The weakest busbar is located as the point(s) of the lowest reactive power margin.

The results are summarized in Table 1, where the six buses with the lowest voltage magnitude (pu) are shown. Kaduna bus has the highest voltage magnitude in both scenarios, 0.93 per unit during the summer and 0.96 per unit during the winter. The lowest QV values during summer and winter are observed at Yola with values of 0.41 per unit and 0.35 per unit, respectively.

3.5 *Active and reactive power results*

Table 2 presents additional results in relation to load flow, PV, and QV analysis for the base case (no HVDC in the network). This table illustrates generated power, load demand, line losses, and reactor output. The sum of active power absorbed by the loads and line losses equals the generated power. The sum of the load reactive power, the line reactive power, and the reactor's output are the same as the generated reactive power.

Table 2. Summary of power flow, PV and QV results for the base case

Base case	Generator		Load		Losses		Reactor	Critical bus	Critical voltage (pu)
	MW	Mvar	MW	Mvar	MW	Mvar	Mvar		
Load flow	4,804	−298	4,654	1,281	150	−2,338	759	-	-
PV	5,663	331	5,399	1,486	264	−1,873	725	Yola	0.66
								Gombe	0.69
QV	4,844	109	4,654	1,281	190	−1,890	718	Yola	0.5
								Gombe	0.41

As a result of load increase during the PV analysis, generated power, load demand and line losses increased by 18%, 16%, and 76%, respectively. From the QV analysis, the power generated increased slightly by 0.83% and line losses by 27%, due to higher currents. According to the load flow analysis, more reactive power (759 Mvar) is required to balance and control the voltage because the loads are inductive.

The static stability study showed that the transmission system's radial feeders are the weakest link because they have a single point of supply. More specifically, both PV and QV analysis indicate that Yola and Gombe are the critical buses, and these two bus bars are now considered for the HVDC connection. The power flow and reliability analysis of this network, presented in [7,21], identified these two buses as having the lowest voltage magnitude and the lowest reliability, respectively.

4. Impact of HVDC on stability analysis

4.1 *Impact of HVDC on PV analysis*

The impact of HVDC on PV analysis is presented for two cases:

• Case 1: HVDC connected between Azura and Gombe.

• Case 2: HVDC connected between Azura and Yola.

The Azura bus has been chosen as the sending end in both cases because of the presence of a larger generator and its distance from the loads. The HVDC length is 1,020 km and 1,025 km for Case 1 and Case 2, respectively. The load flow results, and PV results are summarized in Table 3 (Case 1) and Table 4 (Case 2).

Table 3. Power flow and PV study results for case 1: HVDC connected between azura and gombe

	Generation (MW)	Load (MW)	Losses (MW)	Critical bus	Critical voltage (pu)
Load flow	4,784	4,654	129	-	-
PV study	10,690	8,480	2,210	Kano	0.72

Table 4. Power flow and PV study results for case 2: HVDC connected between azura and yola

	Generation (MW)	Load (MW)	Losses (MW)	Critical bus	Critical voltage (pu)
Load flow	4,788	4,654	133	-	-
PV study	10,475	8,329	2,146	Kano	0.71

The power generated for Case 1 is 4,784 MW, while for Case 2 is 4,788 MW. These results are slightly lower than the base case (4,804 MW, as shown in Table 2). This is partly due to a small decrease in line power loss when the HVDC is in service (21 MW and 17 MW, respectively, for Case 1 and Case 2).

Table 3 reveals that the critical demand improved to 8,480 MW, while Table 4 shows a critical demand of 8,329 MW. The increase equals 3,081 MW and 2,930 MW respectively, compared to the base case (5,399 MW) in Table 2. The generated power was improved by 123% compared to the base case. For Case 2, the generated power was improved by approximately 119%.

Figures 5 and 6 show the PV results for Case 1 and Case 2, respectively. Yola critical voltage improved from 0.66 pu to 0.98 pu for Case 1, and 1 pu for Case 2. Gombe critical voltage improved from 0.69 pu to 1.00 pu for Case 1 and 0.91 for Case 2. As expected, the voltage improves the most at the busses connected to the HVDC. For example, in Figure 6, the voltage magnitude remains constant (1.00 pu) for the Yola bus throughout the load variation, while the Gombe bus voltage magnitude dropped from 0.99 pu to 0.91 pu as the power increased. Both Figures 5 and 6 clearly illustrate the significant increase in system loadability when the HVDC is connected. Figures 7 and 8 summarize the results at the weakest busbars, for Case 1 and Case 2. These results above that both Case 1 and Case 2 increase system voltage stability across the system.

Table 5 summarize the results related to load capability at Gombe and Yola-initial load flow, base case, Case 1 and Case 2. This table illustrates that the HVDC connection allows for a significant increase in demand. Active and reactive power increases at all busses are shown in the appendix, together with the load power factor.

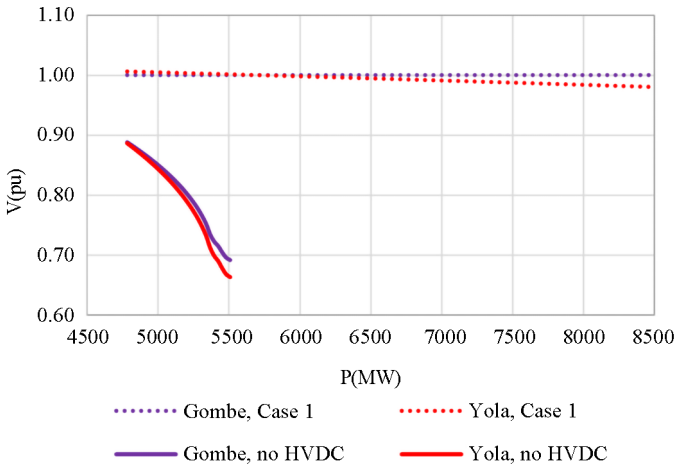


Figure 5. PV curves for gombe and yola for the base case and for case 1

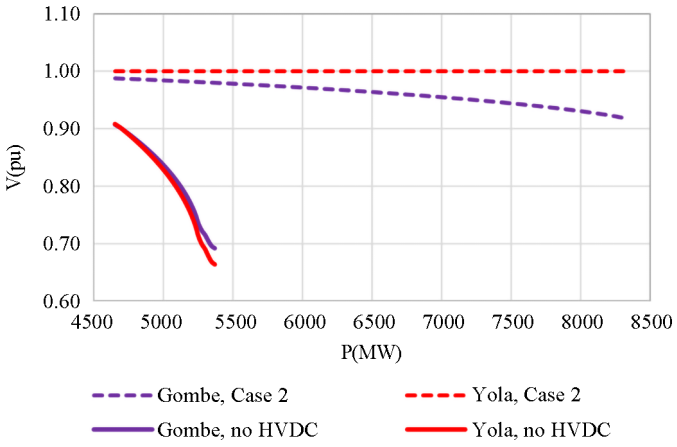


Figure 6. PV curves for gombe and yola for the base case and for case 2

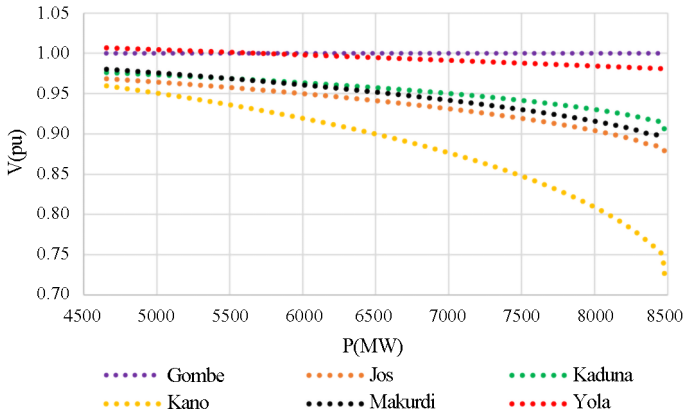


Figure 7. PV curves of the weak buses for case 1

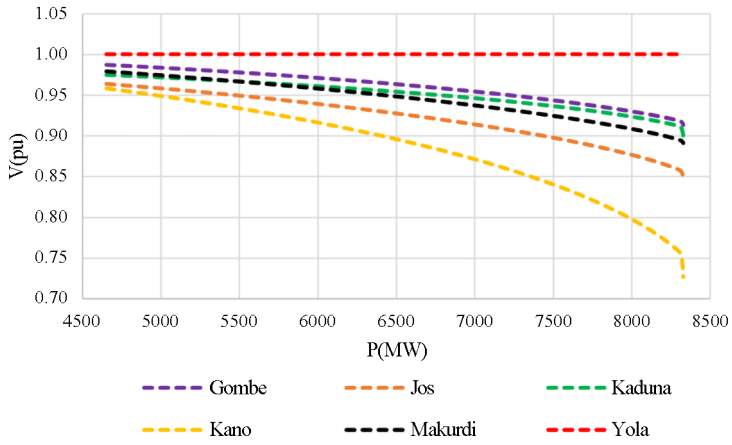


Figure 8. PV curves of the weak buses for case 2

Table 5. Active and reactive power at gombe and yola for initial demand and maximum load

	Initial demand		Maximum load					
			Base case		case 1		case 2	
Bus	P (MW)	Q (Mvar)	P (MW)	Q (Mvar)	P (MW)	Q (Mvar)	P (MW)	Q (Mvar)
Gombe	154	30	179	35	280	55	276	54
Yola	73	26	85	30	133	47	131	47

4.2 *Impact of HVDC on QV analysis*

The impact of HVDC on QV analysis is presented in this section for the two cases considered above. Figure 9 shows the results for Case 1 and Case 2. The voltage at Yola bus improved from 0.91 pu (red continuous curve) to 1.01 pu (red dashed curve), while the reactive power margin (RPM) improved from −43 Mvar to −306 Mvar. The critical point did not improve but it slightly degraded from 0.61 pu to 0.62 pu because power systems' load demand might change during the day and throughout the season (change in load patterns). For Case 2, an improvement is experienced at the Gombe bus.

The operating point moves from 0.91 pu (purple continuous curve) to 0.99 pu (purple dotted curve) while the reactive power margin improves from −54 Mvar to −448 Mvar. The critical point of collapse improved from 0.67 pu to 0.61 pu. This implies that the collapse point is further away with 0.61 pu and, therefore, the loadability of the bus increases. The power transmission capacity, load margin, and losses were all improved for both Case 1 and Case 2.

The impact of HVDC on the QV analysis is summarized in Tables 6 and 7, for Case 1 and Case 2, respectively. It shows that Yola voltage improved from 0.91 pu (base case) to 1.01 pu with a critical point of 0.62 pu. Gombe voltage improved from 0.91 pu (base case) to 0.99 pu with a critical point of 0.61 pu, respectively. Noteworthy, in Case 1, the reactive power on Gombe is 0.02 Mvar at 1.00 pu (Table 6). Similarly, for Case 2, the reactive power on Yola is 0.02 Mvar at 1.00 pu (Table 7). This is because HVDC transmission does not contribute to the reactive power flow at the busbars in the same way as AC transmission [33].

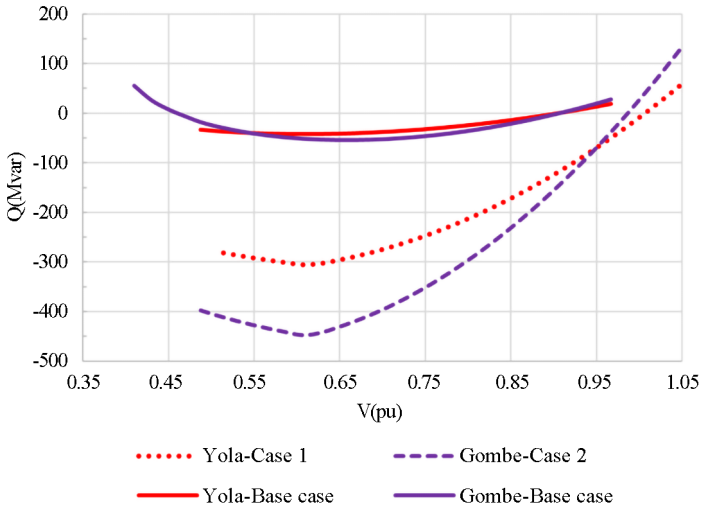


Figure 9. VQ curves for the base case, case 1 and case 2 (for case 1 the curve at gombe reduces to a point, and, conversely, for case 2 the curve at yola reduces to a point, and they are not shown in the graph. The operating points under these conditions are listed in Tables 6 and 7)

Table 6. QV results for case 1

Bus	Operating point		Critical point	
	V (pu)	Q (Mvar)	V (pu)	Q (Mvar)
Gombe	1	0.02	0	0
Yola	1.01	0	0.62	−306

Table 7. QV result for case 2

Bus	Operating point		Critical point	
	V (pu)	Q (Mvar)	V (pu)	Q (Mvar)
Gombe	0.99	0	0.61	−448
Yola	1	0.02	0	0

Figures 10 and 11 shows the results for QV analysis at all buses, for Case 1 and Case 2, respectively. In Figure 10, the operating curve for Gombe reduces to one point, as the HVDC allows controlling the voltage at the busbar is connected

to. Similarly, in Figure 11, the operating curve for Yola reduces to one point. The results indicate that the HVDC interconnections allow for an increase of system RPM across the system.

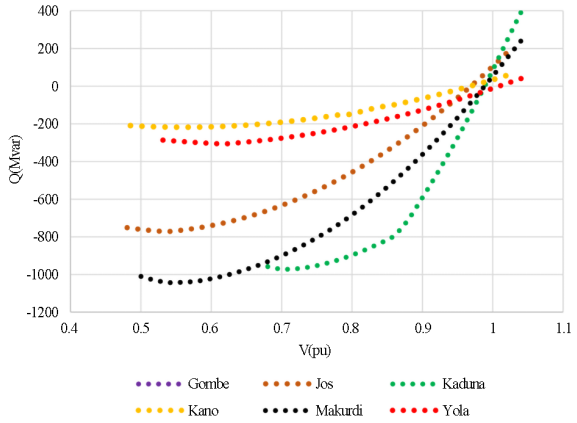


Figure 10. VQ curves for the weak buses for case 1 (for this case, the curve at gombe reduces to an individual point and is not visible on the graph)

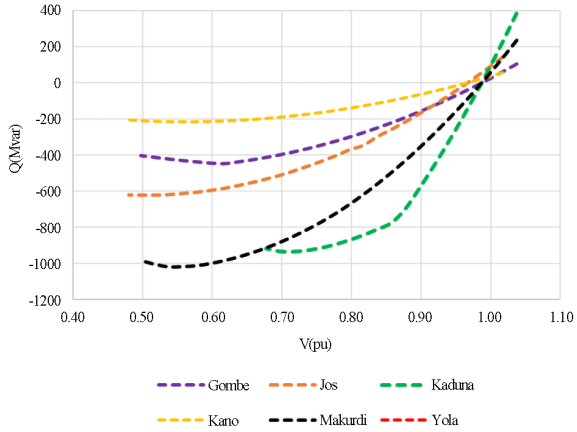


Figure 11. VQ curves for the weak buses for case 2 (for this case, the curve at yola reduces to an individual point and is not visible on the graph)

4.3 *Impact of HVDC with different control modes*

The next step of this analysis investigated the impact of four HVDC control modes on the transmission network. The four control modes were defined in Section 3.2, and are summarized below and referred to as follows:

I: $V_{dc}-Q/P-V_{ac}$,

II: $V_{dc}-\cos\phi_2/P-V_{ac}$,

III: $V_{dc}-\cos\phi_2/P-Q$,

IV: $V_{dc}-Q/P-Q$.

In the next subsections, results for the four control modes are only shown for Case 1, as Case 2 leads to very similar conclusions.

4.3.1 *Load flow results*

The load flow analysis was performed for each control mode, and the results are recorded in Table 8. The generated power was slightly lower (4,788 MW) for all control modes, compared to the case with no HVDC on the network (4,804 MW). The power generated with I and II are the same and, therefore, results in the same losses. The losses with I

and II are lower than the losses without HVDC. Similarly, control modes III and IV have the same generated power (4,787 MW) and losses. The power generated and losses for the four control modes are very similar, therefore, it can be concluded that the control modes did not have a significant effect on the load flow analysis results.

Table 8. Load flow results with different control modes for case 1

		Generation		Losses		Bus voltage	
	Control mode	MW	Mvar	MW	Mvar	Yola (pu)	Gombe (pu)
-	Without HVDC	4,804	−298	150	−2,338	0.91	0.91
I	V_{dc}−Q/P−V_{ac}	4,788	−497	133	−2,560	1	0.99
II	V_{dc}−cosϕ_2/P−V_{ac}	4,788	−497	133	−2,560	1	0.99
III	V_{dc}−cosϕ_2/P−Q	4,787	−517	132	−2,574	1.03	1.01
IV	V_{dc}−Q/P−Q	4,787	−517	132	−2,574	1.03	1.01

Table 9 summarizes the voltage profile at various busbars and show an overall improvement, compared to the base case. The voltages are all within the permissible limit, ranging from 0.95 pu to 1.05 pu.

Table 9. Load flow results at different busbars (voltage) with different control modes for case 1

Bus \ B	Gombe (pu)	Jos (pu)	Makurdi (pu)	Yola (pu)
without HVDC	0.91	0.91	0.96	0.91
I	0.99	0.96	0.98	1.00
II	0.99	0.96	0.98	1.00
III	1.01	0.97	0.98	1.03
IV	1.01	0.97	0.98	1.03

4.4 *PV and QV results*

Table 10 shows the PV and QV analysis results for different control modes. The generation output remains constant across all modes, with a value of 10,475 MW for control modes I and II, and 8,298 MW for control modes III and IV.

Table 10. Case 1: PV and QV analysis result with different control modes

		PV		QV
Control mode	Critical bus	Critical demand (MW)	Critical voltage (pu)	Critical voltage (pu)
No HVDC	Yola	5,398	0.66	0.41
I	Kano	8,329	0.73	0.55
II	Kano	8,329	0.73	0.55
III	Yola	7,362	0.68	0.54
IV	Yola	7,362	0.68	0.54

Therefore, a much higher system loadability can be achieved with control modes I and II, meaning that critical demand increases.

However, it was observed that no significant changes to the QV calculation resulted from using any of the control modes, compared to the base case. This is because, during the QV calculation, the generator power is constant, and the

HVDC adjusts reactive power and voltage levels to the set values. The power generated was 4,784 MW and −556 Mvar with all control modes, the losses were 129 MW and −2,594 Mvar, supplying the same load of 4,654 MW and 1,281 Mvar. The critical bus for the QV calculation remains the same as that of the PV calculation (Kano and Yola) while the critical voltage is shown in Table 10.

5. Contingency analysis

Contingency analysis is used to manage and analyse abnormal conditions in electrical networks, such as sudden changes in transmission lines, generators, or load [34,35]. N-1 contingency is a common standard for assessing the security of power systems-according to this criterion, power system should withstand any single component failure with no violations of operating constrains, while supplying all loads [35]. N-1 contingency analysis was carried out for the Nigerian power system, based on outage data used in a previous work [21].

The contingency considered was to take the line connecting Jos and Gombe out of service. This can be considered as one of the worst cases as these two buses are identified as weak buses in the system from the PV and QV analysis.

Figures 12 and 13 shows the results for contingency analysis for the base case, and for Case 2, respectively. The results for Case 1 are not shown as they are very similar. Figure 12 shows typical PV graphs, but one note that both Jos and Gombe voltage is zero due to the outage. Figure 13 shows a significant improvement at Yola and Gombe due to the presence of the HVDC. Other voltages are not impacted significantly, nevertheless, under nominal load conditions, all voltages are above 0.9 pu.

Therefore, one can conclude that under contingency conditions the HVDC still supports the system, but when considering future system expansion, then other measures should be introduced to guarantee stable operating conditions.

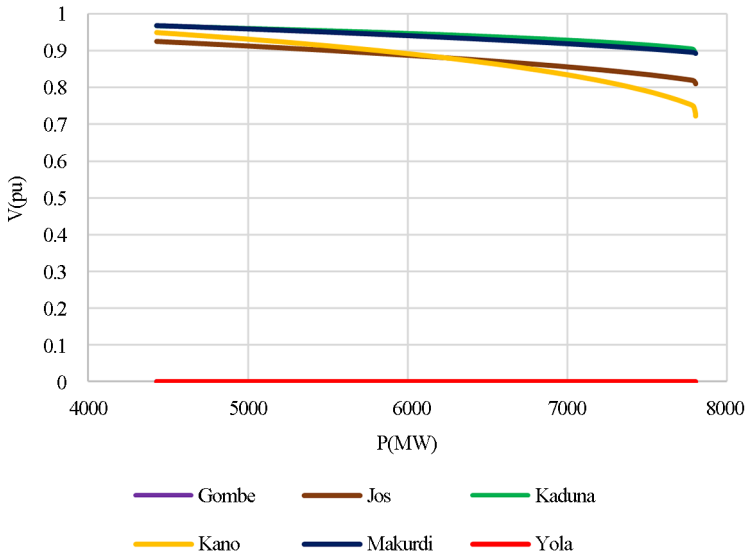


Figure 12. PV graph under N-1 contingency (line jos-gombe out of service) for the base case

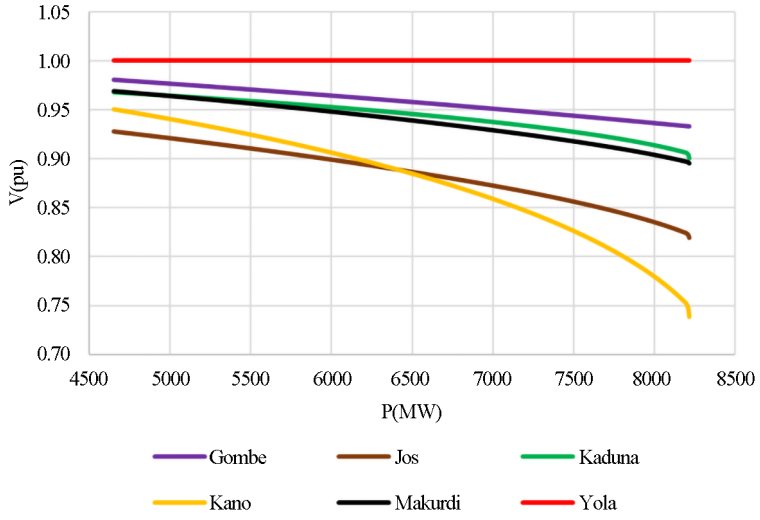


Figure 13. PV graph under N-1 contingency (line jos-gombe out of service) for case 2

6. Conclusions

This work presented a stability analysis of the Nigerian transmission system. A system model was built based on data provided by the Nigeria Electricity System Operator (NESO) from the summer and winter of 2019. Both summer and winter scenarios were established in the DSPF environment. Stability studies were carried out using both PV and QV analysis to determine weak buses on the Nigerian transmission network.

Two sites (Gombe and Yola) were identified as suitable for an HVDC link. Two different HVDC interconnectors (Case 1 and Case 2) were studied, and the results show an improved system reliability for both cases. Following a close inspection of the results, Case 2 resulted in an overall better performance, in both voltage profile and RPM.

Various HVDC control modes were considered, and they all resulted in similar performance in PV and QV analysis results. As a result of this analysis, and previous work carried out on load flow and stability studies, it is concluded that HVDC transmission is a promising approach to address the challenges of losses and instabilities experienced by the Nigerian Transmission Grid. The next steps of this work will include an economic analysis.

Funding

This research was supported by the Tertiary Education Trust Fund (TETFUND) under the Academic Staff Training & Development (AST&D) program of the Federal Republic of Nigeria and by the UK Engineering and Physical Sciences Research Council (EPSRC) grant EP/T013206/2. TETFUND's support in producing this publication does not constitute an endorsement of the contents, which reflect the views only of the authors, and the Commission cannot be held responsible for any use which may be made of the information contained therein.

Acknowledgments

The authors acknowledge the Nigeria Energy System Operator (NESO) for making the data available for this research work and Olabisi Onabanjo University for supporting the research work. Also acknowledge the support given by Dr. Apena Waliu of The Federal University of Technology, Akure, Nigeria. For the purpose of open access, the author has applied for a Creative Commons Attribution (CCBY) license to any Author-Accepted-Manuscript version arising.

Conflict of interest

There is no conflict of interest for this study.

Abbreviation

HVDC	High Voltage Direct Current
DSPF	DIgSILENT PowerFactory
pu	Per unit
PV	Power Voltage
RPM	Reactive Power Margin
NESO	Nigeria Electricity System Operator
QV	Reactive Voltage
VSC	Voltage Source Converter
SVS	Static Var System

Appendix

Table 11. P and Q value for all buses, for four cases

					Maximum load				
	Initial power		Base case		Case 1		Case 2		
Bus	P (MW)	Q (Mvar)	P (MW)	Q (Mvar)	P (MW)	Q (Mvar)	P (MW)	Q (Mvar)	pf
Aja	163	121	189	140	296	220	291	216	0.80
Alagbon	162	75	188	87	295	137	290	134	0.91
Alaoji	415	100	481	117	755	183	742	180	0.97
Ayede	208	25	241	29	379	45	372	44	0.99
B.kebbi	198	3	230	3	360	5	354	5	1.00
Benin	133	121	154	140	242	220	238	216	0.74
Ganmo	80	0	93	0	146	0	143	0	1.00
Gombe	154	30	179	35	280	55	276	54	0.98
Ikeja West	1,135	200	1,317	232	2,066	365	2,031	359	0.98
Jebba-	14	1	16	2	25	3	25	3	1.00
Jos	80	63	93	73	146	115	143	113	0.79
Kaduna	176	0	204	0	320	0	315	0	1.00
Kano	277	0	321	0	504	0	496	0	1.00
Katampe	465	130	539	151	847	237	832	233	0.96
Makurdi	162	131	188	152	295	238	290	234	0.78
New.h	100	15	116	18	182	28	179	28	0.99
Onitsha	142	56	164	65	258	102	253	100	0.93
Osogbo	167	101	194	117	304	184	299	180	0.86
Sakete	226	30	262	35	411	55	404	54	0.99
Sapele	64	48	74	55	117	87	115	85	0.80
Shiroro	62	5	71	6	112	9	110	9	1.00
Yola	73	26	85	30	133	47	131	47	0.94
Total	4,654	1,281	5,399	1,486	8,473	2,333	8,328	2,293	

References

[1] E. Saadati and A. Mirzaei, "Voltage stability indices: Taxonomy, formulation and calculation algorithm," *International Journal of Scientific and Engineering Innovation Research*, vol. 8, pp. 1-6, 2016.

[2] B. Ismail, N. I. A. Wahab, M. L. Othman, M. A. M. Radzi, K. N. Vijayakumar, M. K. Rahmat, et al., "New line voltage stability index (BVSI) for voltage stability assessment in power system: The comparative studies," *IEEE Access*, vol. 10, pp. 103906-103931, 2022. https://doi.org/10.1109/ACCESS.2022.3204792.

[3] B. Badejo, O. Olasunkanmi, and O. Nathaniel, "Investigating electricity consumption in Ogun State, Nigeria," *Journal of Engineering Studies and Research*, vol. 26, 2020.

[4] O. G. Olasunkanmi, P. O. Alao, F. Onaifo, M. O. Osifeko, J. O. Sholabi, "Reliability assessment of a gas generating station in Ogun State, Nigeria," *Journal of Applied Sciences and Environmental Management*, vol. 22, p. 1005, 2018. https://doi.org/10.4314/jasem.v22i6.27.

[5] C. Subramani, S. S. Dash, V. Kumar, and H. Kiran, "Implementation of line stability index for contingency analysis and screening in power systems," *Journal of Computer Science*, vol. 8, pp. 585-590, 2012. https://doi.org/10.3844/jcssp.2012.585.590.

[6] O. G. Olasunkanmi, M. R. Adu, and W. O. Apena, "Enhancing Nigeria's power grid performance through a hybrid transmission network," *Nigerian Journal of Technology Research*, vol. 14, 2019. https://doi.org/10.4314/njtr.v14i2.2.

[7] O. G. Olasunkanmi, Z. Deng, and G. Todeschini, "Load flow analysis of the Nigerian transmission grid using DIgSILENT PowerFactory," In Proc. 56th International Universities Power Engineering Conference (UPEC), Middlesbrough, UK, Aug. 31-Sep. 3, 2021. https://doi.org/10.1109/UPEC50034.2021.9548253.

[8] S. Ratra, R. Tiwari, and K. R. Niazi, "Voltage stability assessment in power systems using line voltage stability index," *Computers and Electrical Engineering*, vol. 70, pp. 199-211, 2018. https://doi.org/10.1016/j.compeleceng.2017.12.046.

[9] N. Hatziargyriou, J. Milanovic, C. Rahmann, V. Ajjarapu, C. Canizares, I. Erlich, et al., "Definition and classification of power system stability-revisited & extended," *IEEE Transactions on Power Systems*, vol. 36, pp. 3271-3281, 2021. https://doi.org/10.1109/TPWRS.2020.3041774.

[10] P. Kundur, J. Paserba, V. Ajjarapu, G. Andersson, A. Bose, C. Canizares, et al., "Definition and classification of power system stability IEEE/CIGRE joint task force on stability terms and definitions," *IEEE Transactions on Power Systems*, vol. 19, pp. 1387-1401, 2004. https://doi.org/10.1109/TPWRS.2004.825981.

[11] M. B. Keskin, "Continuation power flow and voltage stability in power systems," M.S. Thesis, Middle East Technical University, Ankara, Turkey, 2007. https://hdl.handle.net/11511/17086.

[12] S. K. Mazumder and E. P. de la Fuente, "Stability analysis of micropower network," *IEEE Journal of Emerging and Selected Topics in Power Electronics*, vol. 4, pp. 1299-1309, 2016. https://doi.org/10.1109/JESTPE.2016.2592938.

[13] X. Li, Z. Li, L. Guan, X. Wu, Y. Mei, and J. Li, "Study on the corresponding relationship between critical points of P-V curve and V-Q curve of simple Thevenin equivalent system," In Proc. 2020 IEEE 1st China International Youth Conference on Electrical Engineering (CIYCEE), Wuhan, China, Nov. 1-4, 2020. https://doi.org/10.1109/CIYCEE49808.2020.9332740.

[14] O. Mogaka, R. Orenge, and J. Ndirangu, "Static voltage stability assessment of the Kenyan power network," *Journal of Electrical and Computer Engineering*, vol. 2021, pp. 1-16, 2021. https://doi.org/10.1155/2021/5079607.

[15] L. Zhang, H. Lennart, and P. Rey, "Power system reliability and transfer capability improvement by VSC-HVDC," In Proc. CIGRE Regional Meeting 2007, Tallinn, Estonia, Jun. 18-20, 2007, pp. 1-7.

[16] F. Aydin and B. Gumus, "Determining optimal SVC location for voltage stability using multi-criteria decision making based solution: Analytic hierarchy process (AHP) approach," *IEEE Access*, vol. 9, pp. 143166-143180, 2021. https://doi.org/10.1109/ACCESS.2021.3121196.

[17] N. Manjul and M. S. Rawat, "PV/QV curve based optimal placement of static var system in power network using DigSilent Power Factory," In Proc. 2018 IEEE 8th Power India International Conference (PIICON), Kurukshetra, India, Dec. 10-12, 2018. https://doi.org/10.1109/POWERI.2018.8704441.

[18] M. Kirik, "VSC-HVDC for long-term voltage stability improvement," M.S. Thesis, Royal Institute of Technology, Stockholm, Sweden, 2009.

[19] H. F. Latorre and M. Ghandhari, "Improvement of power system stability by using a VSC-HVdc," *International Journal of Electrical Power and Energy Systems*, vol. 33, pp. 332-339, 2011. https://doi.org/10.1016/j.ijepes.2010.08.030.

[20] E. D. Aguero, J. C. Cepeda, and D. G. Colome, "FACTS models for stability studies in DIgSILENT Power Factory," In Proc. 2014 IEEE PES Transmission and Distribution Conference and Exposition-Latin America (PES T&D-LA), Medellin, Colombia, Sep. 10-13, 2014. https://doi.org/10.1109/TDC-LA.2014.6955182.

[21] O. G. Olasunkanmi, W. O. Apena, A. R. Barron, A. O. White, and G. Todeschini, "Impact of a HVDC link on the reliability of the bulk Nigerian transmission network," *Energies*, vol. 15, p. 9631, 2022. https://doi.org/10.3390/en15249631.

[22] B. V. Ramana, K. V. S. R. Murthy, P. U. Kumar, and V. R. Kumar, "A two bus equivalent method for determination of steady state voltage stability limit of a power system," *International Journal of Computational Engineering Research*, vol. 2, pp. 428-434, 2012.

[23] T. He, S. Kolluri, S. Mandal, F. Galvan, and P. Rastgoufard, "Identification of weak locations in bulk transmission systems using voltage stability margin index," In Proc. International Conference on Probabilistic Methods Applied to Power Systems, Denver, CO, USA, Jun. 6-10, 2004. https://doi.org/10.1109/PES.2004.1373193.

[24] V. Ajjarapu, *Computational Technique for Voltage Stability Assessment and Control*, Ames, IA, USA: Springer, 2006, pp. 220-225.

[25] DIgSILENT, *PowerFactory 2020: User Manual*, 2020th ed. Gomaringen, Germany: DIgSILENT GmbH, 2020.

[26] A. G. Simens, "High voltage direct current transmission-proven technology for power exchange," [online]. Available: https://www.ewh.ieee.org/r6/san_francisco/pes/pes_pdf/HVDC_Technology.pdf. [Accessed 12 December 2023].

[27] Y.-C. Kim, L. Jin, J.-M. Lee, and J.-H. Choi, "Direct digital control of single-phase AC/DC PWM converter system," *Journal of Power Electronics*, vol. 10, pp. 518-527, 2010. https://doi.org/10.6113/JPE.2010.10.5.518.

[28] V. G. Csutar, S. Kallikuppa, and L. Charles, "Introduction to HVDC architecture and solutions for control and protection," [online]. Available: https://www.ti.com/lit/an/sloa289b/sloa289b.pdf. [Accessed 19 December 2023].

[29] H. F. Latorre, "Modeling and control of VSC-HVDC transmissions," Ph.D. dissertation, Royal Institute of Technology, Stockholm, Sweden, 2011.

[30] D. M. Mohan, B. Singh, and B. K. Panigrahi, "Analysis, design and control of two-level voltage source converters for HVDC systems," *Journal of Power Electronics*, vol. 8, pp. 248-258, 2008.

[31] D. Rabie, T. Senjyu, S. Alkhalaf, Y. S. Mohamed, and E. Shehata, "Study and analysis of voltage source converter control stability for HVDC system using different control techniques," *Ain Shams Engineering Journal*, vol. 12, pp. 2763-2779, 2021. https://doi.org/10.1016/j.asej.2020.12.013.

[32] DIgSILENT, *DIgSILENT Technical Documentation: PWM Converter*, Gomaringen, Germany: DIgSILENT GmbH, 2020.

[33] NationalgridESO, "Reactive power market design-market analysis," [online]. Available: https://www.neso.energy/about/our-projects/reactive-power-market-design. [Accessed 12 December 2023].

[34] V. J. Mishra and M. D. Khardenvis, "Contingency analysis of power system," In Proc. 2012 IEEE Students' Conference on Electrical, Electronics and Computer Science (SCEECS), Bhopal, India, Mar. 1-2, 2012. https://doi.org/10.1109/SCEECS.2012.6184751.

[35] S. Ahmad, N. M. Zakaria, and G. A. K. Biswas, "Contingency analysis and reliability evaluation of Bangladesh power system," Ph.D. dissertation, BRAC University, Dhaka, Bangladesh, 2011.